GA–A26107

FLUID MODELING OF AN ELMING H-MODE AND A RMP H-MODE

by
S. MORDIJCK, R.A. MOYER, T.E. EVANS, X. BONNIN, J. CANIK, D. COSTER, M. GROTH, R. MAINGI, T.H. OSBORNE, L.W. OWEN, T.W. PETRIE, D. REITER, J.G. WATKINS, and E.A. UNTERBERG

JUNE 2008

GENERAL ATOMICS

DISCLAIMER

GA–A26107

FLUID MODELING OF AN ELMING H-MODE AND A RMP H-MODE

by
S. MORDIJCK,* R.A. MOYER,* T.E. EVANS, X. BONNIN,† J. CANIK,‡ D. COSTER,¶ M. GROTH,§ R. MAINGI,‡ T.H. OSBORNE, L.W. OWEN,‡ T.W. PETRIE, D. REITER,# J.G. WATKINS,△ and E.A. UNTERBERG◊

This is a preprint of a paper to be presented at the Eighteenth International Conference on Plasma Surface Interactions, May 26-30, 2008, in Toledo, Spain, and to be published in the *J. Nucl. Mater.*

*University of California-San Diego, La Jolla, California.
†Laboratoire d'Ingenierie des Materiaux et des Hautes Pressionns – CNR, Villetanuese, France.
‡Oak Ridge National Laboratory, Oak Ridge, Tennessee.
¶Max-Planck Institut fur Plasmaphysik, Garching Germany.
§Lawrence Livermore National Laboratory, Livermore, California.
#Forschungszentrum Juelich, Juelich, Germany.
△Sandia National Laboratories, Albuquerque, New Mexico.
◊Oak Ridge Science Education, Oak Ridge, Tennessee.

Work supported in part by
the U.S. Department of Energy
under DE-FG03-07ER54917, DE-FG02-05ER54809, DE-FC02-04ER54698,
DE-AC05-00OR22725, DE-AC52-07NA27344, DE-AC04-94AL85000,
and DE-AC05-76OR00033

GENERAL ATOMICS ATOMICS PROJECT 30200
JUNE 2008

GENERAL ATOMICS

Abstract

In this paper we investigate the role of wall conditions during the density pump-out observed in Resonant Magnetic Perturbation (RMP) experiments. We use a 2D fluid code, coupled to a neutral Monte-Carlo code (SOLPS5) to model a reference ELMing H-mode. Next we modify either the recycling at the target plates or the pumping efficiency at the pump entrance. This causes a change in upstream profiles, that alone cannot account for the shape change observed in the RMP H-mode. Therefore, the radial transport must be altered to match the RMP H-mode. By comparing the transport model for the ELMing H-mode and the RMP H-mode, we show that inside the separatrix an increase in transport is necessary to model the effects of the applied perturbed field in RMP H-mode.

I. INTRODUCTION

Edge localized modes (ELMs) are predicted to exceed a critical heat load, that could lead to serious erosion of the target plates in ITER.[1,2] Reducing the impulsive power loading at the divertor target plates due to ELMs is therefore critical to the operation of ITER. Recently it has been shown that resonant magnetic perturbations (RMP) successfully suppress ELMs,[3] by lowering the pressure gradient below the peeling-ballooning stability limit.[4] The density pump-out observed in RMP experiments is the prime factor for lowering the pressure gradient.

In this paper we investigate the effects of wall conditions and pumping with respect to the density pump-out observed during RMP experiments on DIII-D. When the I-coil (a non-axisymmetric coil set with two rows of six coils each[3]) is energized with $n = 3$ magnetic perturbations in a low collisionality regime, density pump-out occurs, and as a result the divertor conditions change,[5] i.e., a lower density strike-point, and a broadening of the density profile on the divertor targets. In high collisionality regimes, ELM suppression is also observed, but there is typically very little or no density pump-out and mid-plane profiles are constant[6]. The profile changes observed in high collisionality as well as low collisionality do not follow theoretical predictions for enhanced magnetic diffusion based upon stochastic magnetic fields[7]. Also, because of high rotation, there are concerns that the plasma might screen the fields which does not allow penetration of the perturbations and limits the formation of a stochastic layer[8].

RMPs introduce strike-point splitting and 3D structures in the divertor[9]. Therefore the amount of plasma wetted area changes, which alters recycling at the target plates, and can lower the pedestal density.[10] In addition, the location of the strike-point determines the pumping efficiency, e.g., moving the strike-point closer to the pump entrance increases the pumping efficiency,[11] splitting may affect pumping.. We therefore investigate whether profile changes upstream are the consequence of strike-point splitting and changes in divertor conditions, or if a change in pedestal transport is required.

To distinguish between the effects of strike-point splitting and transport, we use a 2D fluid code coupled to a Monte Carlo neutral code.[12] In the last decade, several parallel versions of this code have been developed and in this paper SOLPS5[13] is employed. Starting from a reference ELMing H-mode, the transport coefficients are computed, and remain fixed for the remainder of the numerical experiment. In order to validate the simulated effects of strike-point splitting, we scan a predefined range of either the recycling coefficients (0.91-0.97) for the target plates or the pumping efficiency (10%-90%) at the plenum entrance of the cryopump. For all numerical

results, we observe a drop in the midplane density profile ,while its shape remains relatively constant. In contrast, the experimental results show a change in the shape of the density pedestal. Therefore, a change in transport is required to induce this change. Transport inside the separatrix has to increase in the area of the transport barrier to simulate the large drop in density of the pedestal, while keeping a nearly similar density in the scrape-off layer (SOL).

The main results of this paper show how the divertor conditions affect midplane profiles. Also, we show that reduced recycling at the target plates and better pumping efficiency does not solely account for the change in the density pedestal shape observed during RMP experiments.

II. METHOD

This section describes the relevant experimental data and the modeling approach. First, we introduce the experimental setup and most important results. Next, we describe the process followed for the numerical experiments.

To distinguish between a standard ELMing H-mode, which will serve as a reference, and an RMP H-mode, two experiments are carefully selected. The RMP H-mode has exactly the same setup as the reference H-mode, except for the activation of the I-coil at 2000 ms (3.2 kA). The two discharges evolve differently subsequent to the I-coil turn-on. Thus, experimental data is identical for both shots up to 2000 ms (Fig. 1). Comparing both experiments after switching on the I-coil, shows differences on a short time scale, i.e., 50 ms, and on a longer scale, i.e., 300 ms. Three rapid ELMs are observed in the divertor of the RMP H-mode, within the first 50 ms after switching on the I-coil, together with a pressure increase under the baffle. Additionally, a sudden drop in the line-averaged density and an increase in D_α light at both target plates is observed. The line-averaged density continues decreasing for an extended period of time, up to 300 ms after RMP initialization. The pressure under the baffle decreases in a similar fashion, similar to the D_α light at the outer strike-point. On the other hand, the D_α emission at the inner strike-point increases compared to the ELMing H-mode. The changed D_α and pressure imply a change in the recycling coefficients and pumping efficiency.

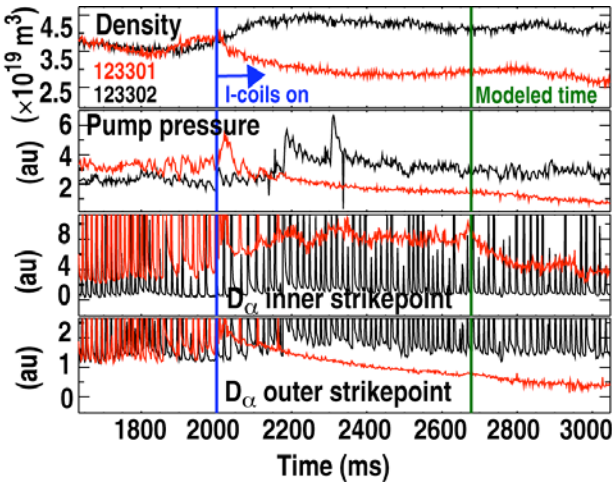

Fig. 1. Experimental results for the ELMing H-mode (black) and the RMP H-mode (red). Time traces include: (a) line averaged density, (b) pressure in the pumping plenum, (c) D_α light at the inner strike point, (d) D_α at the outer strike point.

To understand the effects of recycling at the target plates and of the pumping efficiency, we select a time slice to model, where most variables are relatively stable in the ELMing H-mode (with exception of the ELMs) and the RMP H-mode, namely

at 2675 ms (Fig. 1). This time slice is located between two ELMs for the ELMing H-mode. Also, the transient behavior caused by the ELMs is not modeled. Next, we construct a grid (48 by 96), based on the equilibrium data of the ELMing H-mode. To derive the transport model, we apply the same techniques discussed in Ref. 14. At the core boundary, fixed density and temperatures (the temperature results are not discussed in this paper) are chosen as boundary conditions based on experimental data. This boundary condition limits how the profiles react in its neighborhood. Because of the fixed density, the density gradient changes in this area to accommodate for the changes in flux created by changing the divertor conditions. However if a fixed flux would have been chosen, the effect would have been the opposite. The density would have changed, whereas the density gradient would have been fixed. The SOL and private flux region (PFR) boundary conditions are characterized by short decay lengths (of the order of a few cm), allowing poloidal variation of the effective values. The Bohm-Chodura sheath boundary condition is used at the target plates. Boundary conditions for EIRENE are the recycling coefficients, which are set to 1 everywhere, with the exception of the target plates where 0.97 is used. The pumping efficiency is set at the opening under the baffle at a value of 30%. The transport model is varied until the modeled profiles are comparable to the experimental profiles. The final transport model is fixed for the subsequent numerical experiments.

Our numerical experiment starts by reducing the recycling in the divertor at both target plates and we examine the effect on the upstream profiles by comparing the numerical profiles to the experimental data from the ELMing H-mode. Then, in a similar fashion the pumping efficiency is independently altered and profiles are again compared with the ELMing H-mode. Finally, we model the RMP H-mode by changing the transport model to fit the changed pedestal structure. A comparison of the transport model from the ELMing H-mode with the transport model of the RMP H-mode gives an indication of the effect of the applied magnetic perturbations.

All simulations are performed without drifts and impurities. To simulate the influence of carbon, an artificial radiation coefficient is set at 2% over the whole vessel. Also, all the results are obtained with a radial outward velocity pinch of v = 4.5 m/s. Also, when matching the ELMing H-mode and the RMP H-mode, the thermal transport is adapted to match temperature profiles.

III. RESULTS AND DISCUSSION

In this section, we first discuss the resulting transport model for the ELMing H-mode. Next, the results for the numerical experiments are detailed. Finally, we discuss the comparison of the two transport models.

A. Transport Model ELMing H-mode

The transport model is derived by matching the experimental midplane profiles. Figure 2 shows the measured electron density with experimental error-bars (in red). The solid blue curve is the fitted SOLPS5 data. The values for the particle diffusivity, D_n, k_e are the same magnitude as Gulejova et al. [14] and comparable to commonly used estimates, i.e. 0.2 in the core, a transport barrier and 0.7 at the outer edge of the SOL. Note that only one probe measurement is available near the outer strike-point. The peak values given by our simulation are within a factor of 2 to 3 of the probe measurements.

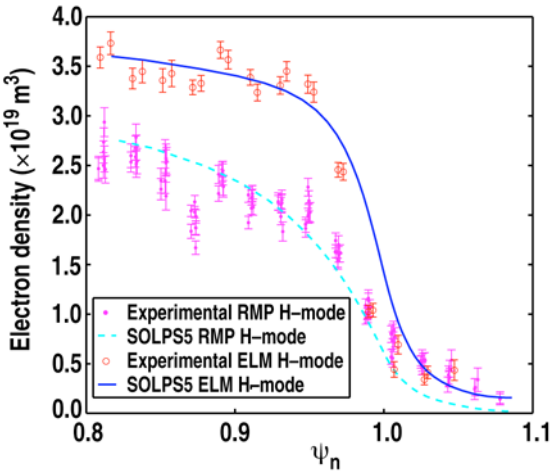

Fig. 2. Density profiles at the midplane. Experimental data for the ELMing H-mode is represented in red and the corresponding SOLPS5 data in blue. Experimental data for the RMP H-mode is represented in magenta and the corresponding SOLPS5 data in cyan.

B. Numerical Experiments

After fixing the transport model, and changing the recycling coefficient at the target plates from 0.97 to 0.95, 0.93 and 0.91, a reduction in the divertor density profile is observed. Moreover, this reduction also manifests itself upstream in the midplane density profile (Fig. 3). The whole density profile, drops with reduced recycling in the divertor. This can be explained by an increased number of plasma particles that are now captured in the target plates, instead of being recycled as

neutrals, which can re-ionize and fuel the core. However, we observe that only changing the recycling at the target plates is not enough to reach RMP H-mode conditions:

1. The peak density at the target plate only drops by a factor 1.5 in the numerical results compared to a factor 3 in the experiment.
2. The midplane density profile change is not large enough and falls within the error bars of the ELMing H-mode.

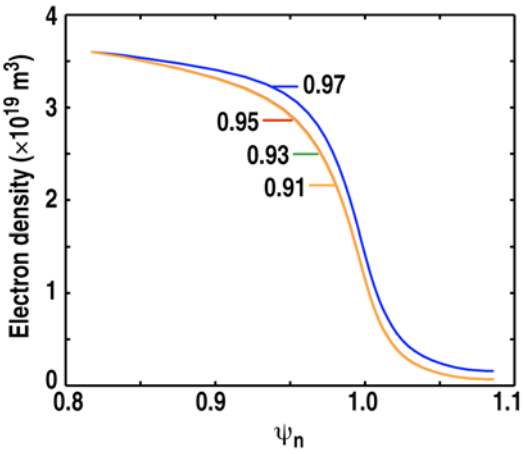

Fig. 3. Calculated dependence of the midplane density profile on recycling coefficient (0.91, 0.93, 0.95 and 0.97) at the target plates. The profiles created by the recycling coefficients 0.91, 0.93 and 0.95 are similar and cannot be distinguished separately in this figure.

Changing the pumping efficiency from 0%-100% shows again the importance of neutral fueling. The numerical runs can become unstable with the chosen core boundary conditions if too few neutrals are pumped from the divertor area. Similarly, pumping more particles not only reduces the density distribution in the divertor, but also reduces the profiles at the midplane (Fig. 4). The reduction is more substantial for increased pumping efficiency when compared to changing the recycling at the target plates.

1. In the divertor, a drop of a factor 4 is observed when going from 30% pumping to 90% pumping.
2. In the divertor, an increase is observed of a factor 2, when going from 30% pumping to only 10% pumping.
3. The change in the shape of the density profile at the midplane is insufficient and saturates.

Comparing these reductions to experimental data shows that we cannot achieve RMP H-mode conditions by only changing the wall conditions in the divertor. Modeling indicates that the pump, which has the biggest effect, needs to increase its efficiency in order to match experiment, whereas experimental data shows a decrease

of particles in the pump (Fig. 1). When comparing particle balances for these two experiments, during I-coil operation the pump in the RMP H-mode pumps three times less particles than the ELMing H-mode, i.e., 9.5 vs 30.9 torr liters. During the same time period, the neutral beams fuel the plasma with about 45 torr liters.

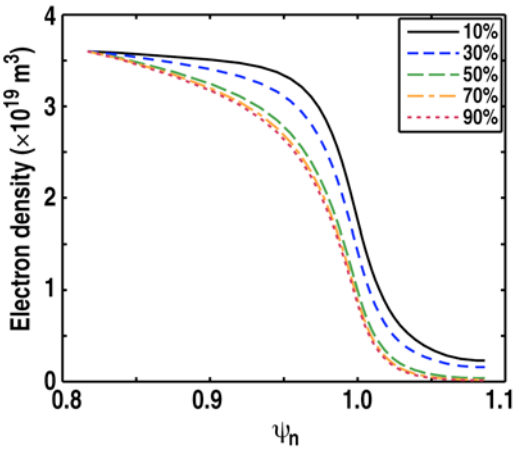

Fig. 4. Calculated dependence of the midplane density profile on pumping efficiency (10%, 30%, 50%, 70% and 90%) at the pump plenum opening.

More important however is that changing the recycling and the pumping efficiency does not alter the pedestal shape, which remains steep, whereas the RMPs modify the pedestal shape. Therefore, the RMP H-mode necessitates a new transport model.

C. Transport Model RMP H-mode

Figure 2 shows the results for the RMP H-mode. The solid cyan line represents the modeled data and the magenta dots the experimental. To achieve these results, the altered transport model is shown in Fig. 5. In the same figure, the transport model for the ELMing H-mode is also displayed. The error bars in Fig. 5 represent the variation in transport coefficients that is consistent with the variation in measured density profiles.

Between y_n of 0.8 and 0.9, both diffusion coefficients are comparable. From $y_n = 0.9$ to 1.0, the transport model for the ELMing H-mode exhibits a barrier. This barrier is needed to obtain the steep density profile just inside the separatrix, whereas the density profile for the RMP H-mode is much more gradual and does not require this reduction in diffusion. At $y_n = 1.1$ both curves cross. In this region, the diffusion coefficient is dominated by parallel SOL flows and the ionization of neutrals and this crossing is not an effect of the RMP.

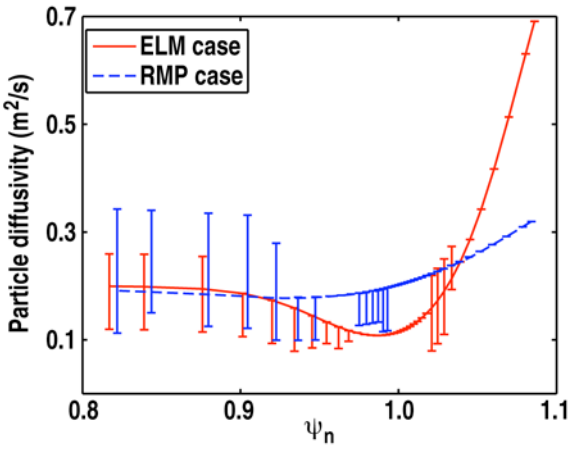

Fig. 5. The particle diffusivity is plotted at the midplane for the ELMing H-mode (blue) and the RMP H-mode (red). Transport in the RMP H-mode is enhanced in the region of the transport barrier calculated for the ELMing H-mode.

IV. CONCLUSION

In this paper, we computed transport coefficients for an ELMing H-mode for the DIII-D tokamak. Next, we showed that reduced recycling in the divertor, not only reduces the density distribution in the divertor, but also in the upstream profiles. Furthermore, we showed that increasing pumping efficiency has a similar, but more pronounced, effect. However, we showed that these effects are not enough to account for the changes observed in the RMP H-mode. The altered wall conditions did not modify the shape of the density pedestal as observed in RMP H-mode experiments. Therefore, the transport model was changed. Comparing the transport model for the RMP H-mode with the transport model for the ELMing H-mode shows enhanced transport inside the separatrix. This enhanced transport is the result of the penetration of perturbed magnetic field lines.

REFERENCES

[1] P. B. Editors, Nucl. Fusion **39** (1999) 2137.
[2] K. Ikeda, Nucl. Fusion **47** (2007) S1.
[3] T. E. Evans, et al., Phys. Plasmas **13** (2006) 056121.
[4] P. B. Snyder, *et al.,* Phys. Plasmas **9** (2002) 2037.
[5] J. G. Watkins, *et al.*, J. Nucl. Mater. **363-365** (2007) 708.
[6] T.E. Evans, *et al.,* Phys. Rev. Lett. **92** (2004) 235003-1
[7] T.E. Evans, *et al.,* Nature of Phys. **2** (2006) 419
[8] R. Fitzpatrick, Phys. Plasmas **5** (1998) 3325.
[9] I. Joseph, *et al.,* Nucl. Fusion **48** (2008) 045009.
[10] R. Maingi, *et al.*, Nucl. Fusion **36** (1996) 245.
[11] R. Maingi, *et al.,* Nucl. Fusion **39** (1999) 1187.
[12] D. Reiter, J. Nucl. Mater. **196-198** (1992) 80.
[13] R. Schneider, *et al.,* Contrib. Plasma Phys. **40** (2000) 328.
[14] B. Glejova, *et al.*, J. Nucl. Mater. **363-365** (2007) 1037.

Acknowledgment

This work was supported in part by the US Department of Energy under DE-FG02-07ER54917, DE-FG02-05ER54809, DE-FC02-04ER54698, DE-AC05-00OR22725, DE-AC52-07NA27344, DE-AC04-94AL85000, and DE-AC05-76OR00033. Special thanks to Pieter Peers.